2016 American Control Conference (ACC)
Boston Marriott Copley Place
July 6-8, 2016. Boston, MA, USA

Robust Power Flow Control of Grid-tied Inverters Based on the Uncertainty and Disturbance Estimator

Yeqin Wang, Beibei Ren, and Qing-Chang Zhong

***Abstract*—In this paper, an uncertainty and disturbance estimator (UDE)-based control is proposed to achieve accurate power flow control for grid-tied inverters (GTI). The power delivering dynamics is introduced at first after considering both frequency dynamics and voltage dynamics. Then the UDE algorithm is adopted to regulate both output voltage amplitude and frequency for accurate real power and reactive power control. With the adoption of the UDE method, the model uncertainty (e.g., power angle) and external disturbance (e.g., variations of grid frequency and grid voltage) can be compensated automatically. Moreover, this UDE-based dynamic power flow control can achieve self-synchronization without an extra synchronization unit (e.g., a phase-locked-loop) when the inverter is connected to the grid. In addition, the proposed controller is easy for implementation and parameter tuning through the designs of desired tracking error dynamics and UDE filters, while having the flexibility and performance of advanced control methodologies. The asymptotic stability of the closed-loop system is analyzed. Experimental results are provided for validation.**

I. Introduction

Nowadays, renewable energies, such as wind energy, solar energy, wave tidal energy and fuel cells, play very important roles in energy area. According to REN21's "Renewables 2015 Global Status Report", the renewable electricity shares 22.8% of global electricity production, with the wind power about 3.1%, and the solar PV (photovoltaic) about 0.9%. According to the reports of U.S. Department of Energy, wind energy is targeted to provide 20% of U.S. electricity needs by 2030, and solar power is targeted to provide 14% of U.S. electricity needs by 2030 and 27% by 2050. Most of the renewable energies are comprised of variable-frequency ac sources (such as wind turbines), high frequency AC sources (such as small gas turbines), or DC sources (such as solar PVs). The DC/AC converters, also called inverters, are needed to interface these renewable energies with the public-utility grid [1]. Though renewable energies are quite popular, there are still some challenges faced by the inverter control for grid integration. For example, the renewable energies, such as wind power, solar PV are not stable energies in different wind conditions or sunlight conditions; the current injected into the grid should be clean sinusoidal to keep system stable and grid friendly [1]; the grid variations (frequency variation or voltage variation), even though they are small, also affect the system stability.

The vector control, originally proposed for the control of electrical machine [2], is a popular control algorithm for three-phase grid-tied inverters (GTI) [3], [4], [5] to convert DC power to AC grid. In the vector control, the current regulation in $d-q$ reference frame is adopted to generate voltage reference. An extra synchronization unit, e.g. the phase-locked-loop (PLL), is required for transformations of current and voltage between the $a-b-c$ reference frame and the $d-q$ reference frame. However, the vector control has its fundamental limitations in power flow control for three-phase GTI. Firstly, the frequency dynamics are not considered in the vector control, which makes it difficult to analyze the angle and frequency stability between GTI and the grid [6]. Secondly, the PLL dynamics can affect the stability of GTI, particularly in weak grids [6], [7]. Moreover, because the PLL is inherently nonlinear and so are the inverter controller and the power system, it is extremely difficult and time-consuming to tune the PLL parameters to achieve satisfactory performance [8]. Thirdly, the instability of the DC-link dynamics can also affect the stability of GTI [6]. Furthermore, the transformation processes of vector control can be complicated due to impedance imbalance and voltage imbalance [9].

An alternative control strategy of the vector control, direct-power control, proposed by [10], directly controls the power switch device based on the instantaneous real power and reactive power errors. This instantaneous control method is easily influenced by system noises, as well as the grid variations. The droop control method, originally proposed for power sharing among parallel operated inverters [11], can be adopted for GTI to achieve power flow control [12], [13], [14], [15]. Though some merits have been achieved with droop control methods, such as harmonic current regulation [12], flexible operation in either grid-connected mode or islanded mode [13], [15], enhancing power loop dynamics [14], the extra synchronization units, the PLLs, are still needed in most cases [12], [14], [15], and frequency dynamics are not considered. As the droop control is based on approximate linearization with the assumptions that the output impedance of the inverter is purely inductive and the power angle is small [1], most droop control strategies are

Yeqin Wang is with the National Wind Institute, Texas Tech University, Lubbock, TX 79409-1021, USA. (e-mail: yeqin.wang@ttu.edu).

Beibei Ren is with the Department of Mechanical Engineering, Texas Tech University, Lubbock, TX 79409-1021, USA. (e-mail: beibei.ren@ttu.edu).

Qing-Chang Zhong is with the Department of Electrical and Computer Engineering, Illinois Institute of Technology, Chicago, IL 60616, USA. (e-mail: zhongqc@ieee.org).

978-1-4673-8681-4/$31.00 ©2016 AACC

static [16].

Inverters can also be controlled to behave as virtual synchronous machines (VSM) [17], [18], [19]. The self-tuning algorithms for optimal parameters of VSM are studied in [20], however, the PLL is still needed in this method. The synchronverter technology [19] has been improved without a dedicated synchronization unit to improve system performance and reduce complexity in [8]. Similar methods have been expanded to introduce the inertia to the grid [6] and to improve microgrids stability [7].

In this paper, a power flow control strategy based on the uncertainty and disturbance estimator (UDE) method is developed for GTI to achieve real and reactive power output regulations. The UDE control algorithm, which was first proposed in [21], is based on the assumption that the uncertainty and disturbance can be estimated by using a filter with the appropriate bandwidth. In recent years, the UDE-based control demonstrated excellent performance in handling uncertainties and disturbances in different systems, and was successfully applied to robust trajectory tracking [22], a class of non-affine nonlinear systems [23], and the variable-speed wind turbine control [24]. In this paper, the power delivering dynamics are studied base on the power delivering equations. Then the UDE-based dynamic power flow control is developed to regulate both output frequency and output voltage for accurate power flow control with self-synchronization when the inverter is connected to the grid. The model uncertainty (e.g., power angle) and external disturbance (variations of grid frequency and grid voltage) can be compensated automatically with this UDE-based dynamic power flow control. Also, this control approach is easy for implementation and parameter tuning with the simple designs of desired tracking error dynamics and UDE filters. The effectiveness of the proposed control approach is demonstrated through experimental studies on an experimental test rig with a single-phase Texas Instruments L-inverter.

The main contributions of this paper are highlighted as follows:

1) The power delivering dynamics are introduced based on the power delivering equations with both frequency dynamics and voltage dynamics being considered.

2) The UDE method is applied for GTI to achieve accurate real and reactive power output regulations. The model uncertainty (e.g., power angle) and external disturbance (variations of grid frequency and grid voltage) can be compensated automatically with UDE algorithm. The self-synchronization is achieved without an extra synchronization unit (e.g., the PLL).

3) The asymptotic stability criteria for GTI with the UDE-based dynamic power flow control is provided.

4) The UDE-based dynamic power flow control is easy to be implemented and tuned while bringing good robust performance.

The rest of this paper is organized as follows. Section II provides power delivering dynamics. In Section III, the UDE-based dynamic power flow is proposed for L-inverter. Effectiveness of the proposed approach is demonstrated through experimental studies in Section IV, before the concluding remarks are made in Section V.

II. Power delivering dynamics

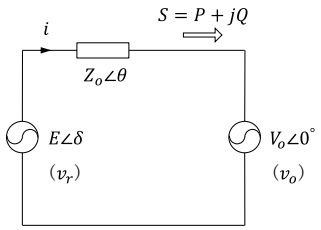

Figure 1. Voltage source delivering power to the grid.

A voltage source $E\angle\delta$ delivering power to the grid $V_o\angle 0^\circ$ through an impedance $Z_o\angle\theta$ can be modeled as shown in Fig. 1. The real power P and the reactive power Q received by the grid $V_o\angle 0^\circ$ are shown as [1]

$$P = \left(\frac{EV_o}{Z_o}\cos\delta - \frac{V_o^2}{Z_o}\right)\cos\theta + \frac{EV_o}{Z_o}\sin\delta\sin\theta, \quad (1)$$

$$Q = \left(\frac{EV_o}{Z_o}\cos\delta - \frac{V_o^2}{Z_o}\right)\sin\theta - \frac{EV_o}{Z_o}\sin\delta\cos\theta, \quad (2)$$

where δ is the phase difference between the voltage source and the grid, often called the power angle.

It is noted that the power delivering equations (1) and (2) are modeled with a general voltage source delivering power to the grid in Fig. 1. This general voltage source could be a GTI or a traditional synchronous generator. The traditional synchronous generators hold the same power delivering characteristics with GTI, though the power delivering equations have little difference [25]. Moreover, sine functions in power delivering characteristics play crucial roles for synchronization and transient stability in power network [26], [27]. If the controller design of GTI follows this power delivering equations, the power delivering characteristics of GTI can obtain the same as traditional synchronous generators, and the same self-synchronization and transient stability of traditional synchronous generators will also be achieved for the operation of the GTI.

Similar to the winding inductance in synchronous generators, because of the output inductor or the inductive line impedance, the output impedance of inverters is mostly inductive and such inverters are called $L-$inverters [1]. In this case, the output impedance of the inverter is considered as purely inductive for simplification with

$$\theta = 90^o.$$

The real power and the reactive power can be derived from (1) and (2) as

$$P = \frac{EV_o}{Z_o}\sin\delta, \quad (3)$$

$$Q = \frac{EV_o}{Z_o}\cos\delta - \frac{V_o^2}{Z_o}. \quad (4)$$

Taking the derivative form of (3) and (4)

$$\dot{P} = \frac{EV_o}{Z_o} cos\,\delta\dot{\delta} + \frac{V_o}{Z_o} sin\,\delta\dot{E}, \quad (5)$$

$$\dot{Q} = \frac{EV_o sin\,\delta\dot{\delta} + V_o\dot{E}cos\,\delta}{Z_o}. \quad (6)$$

Since the power angle δ depends on the power output of the inverter and the variation of grid conditions, it is quite uncertain. The power delivering dynamics (5) and (6) can be rewritten as

$$\dot{P} = \frac{EV_o}{Z_o}\dot{\delta} + \triangle_p, \quad (7)$$

$$\dot{Q} = \frac{V_o}{Z_o}\dot{E} + \triangle_q, \quad (8)$$

where

$$\triangle_p = \frac{V_o}{Z_o} sin\,\delta\dot{E} + \frac{EV_o}{Z_o}\dot{\delta}(cos\,\delta - 1), \quad (9)$$

$$\triangle_q = \frac{EV_o sin\,\delta\dot{\delta}}{Z_o} + \frac{V_o}{Z_o}\dot{E}(cos\,\delta - 1) \quad (10)$$

represent the uncertainty terms, including the nonlinearity and uncertainty of the power angle δ. In practice, the lumped uncertain terms $\triangle_p$ and $\triangle_q$ can be small and bounded because of the small power angle δ.

III. UDE-BASED DYNAMIC POWER FLOW CONTROL

In this paper, a power flow control is proposed based on the power delivering dynamics (7) and (8) with the UDE method [21] for L-inverter. The structure is shown in Fig. 2.

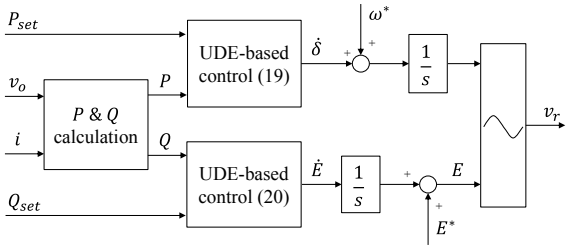

Figure 2. The scheme of the UDE-based dynamic power flow control

A. Controller design

The inverter should accurately control real power and reactive power injected into the grid independently. The control objective is to achieve accurate real power and reactive power regulations, such that real power P and reactive power Q asymptotically track their reference P_{set} and Q_{set} respectively. In particular, the desired tracking errors $e_p = P_{set} - P$ and $e_q = Q_{set} - Q$ satisfy the dynamic equations

$$\dot{e}_p = -K_p e_p, \quad (11)$$

$$\dot{e}_q = -K_q e_q. \quad (12)$$

Combing (7) and (11), (8) and (12) respectively, then

$$\dot{P}_{set} - \frac{EV_o}{Z_o}\dot{\delta} - \triangle_p = -K_p e_p,$$

$$\dot{Q}_{set} - \frac{V_o}{Z_o}\dot{E} - \triangle_q = -K_q e_q.$$

Then $\dot{\delta}$ and $\dot{E}$ need to satisfy

$$\dot{\delta} = \frac{Z_o}{EV_o}\left(\dot{P}_{set} + K_p e_p - \triangle_p\right), \quad (13)$$

$$\dot{E} = \frac{Z_o}{V_o}\left(\dot{Q}_{set} + K_q e_q - \triangle_q\right). \quad (14)$$

According to the system dynamics in (7) and (8), the uncertainty terms $\triangle_p$ and $\triangle_q$ satisfy

$$\triangle_p = \dot{P} - \frac{EV_o}{Z_o}\dot{\delta},$$

$$\triangle_q = \dot{Q} - \frac{V_o}{Z_o}\dot{E}.$$

Following the procedures provided in [21], $\triangle_p$ and $\triangle_q$ can be estimated by

$$\hat{\triangle}_p = (\dot{P} - \frac{EV_o}{Z_o}\dot{\delta}) * g_{pf}, \quad (15)$$

$$\hat{\triangle}_q = (\dot{Q} - \frac{V_o}{Z_o}\dot{E}) * g_{qf}, \quad (16)$$

where " $*$ " is the convolution operator, $g_{pf}(t)$ and $g_{qf}(t)$ are the impulse response of strictly proper stable filters $G_{pf}(s)$ and $G_{qf}(s)$ with unity gain and zero phase shift over the spectrum of the lumped uncertain term $\triangle_p$ and $\triangle_q$ respectively, and zero gain elsewhere. Replacing $\triangle_p$ and $\triangle_q$ with $\hat{\triangle}_p$ and $\hat{\triangle}_q$ in (13) and (14) results in

$$\dot{\delta} = \frac{Z_o}{EV_o}\left[\dot{P}_{set} + K_p e_p - (\dot{P} - \frac{EV_o}{Z_o}\dot{\delta}) * g_{pf}\right], \quad (17)$$

$$\dot{E} = \frac{Z_o}{V_o}\left[\dot{Q}_{set} + K_q e_q - (\dot{Q} - \frac{V_o}{Z_o}\dot{E}) * g_{qf}\right]. \quad (18)$$

Then the UDE-based control laws are formulated as

$$\dot{\delta} = \frac{Z_o}{EV_o}\left[L^{-1}\left\{\frac{1}{1-G_{pf}(s)}\right\} * (\dot{P}_{set} + K_p e_p) - L^{-1}\left\{\frac{sG_{pf}(s)}{1-G_{pf}(s)}\right\} * P\right], \quad (19)$$

$$\dot{E} = \frac{Z_o}{V_o}\left[L^{-1}\left\{\frac{1}{1-G_{qf}(s)}\right\} * (\dot{Q}_{set} + K_q e_q) - L^{-1}\left\{\frac{sG_{qf}(s)}{1-G_{qf}(s)}\right\} * Q\right]. \quad (20)$$

The final controller output v_r for PWM (pulse width modulation) signals generation can be obtained after combining the amplitude obtained from E and the phase δ, as shown in Figure 2.

The UDE-based dynamic control laws (19) and (20) are easy to be implemented and tuned with the simple designs of desired tracking error dynamics and UDE filters. Also, there is no need with an extra synchronization unit for the UDE-based dynamic power flow control when the inverter is

connected to the grid, and the global settings ω^* and E^* are just used for initial synchronization.

It is worth noting that the uncertainty terms $\triangle_p$ (9) and $\triangle_q$ (10) only include the model uncertainty of the power angle δ in the $L-$inverter (with $\theta = 90^o$). If the output impedance of the inverter is not purely inductive, the deviation can also be lumped into the uncertainty terms $\triangle_p$ and $\triangle_q$, which can be estimated and compensated by UDE algorithm. Therefore, the UDE-based dynamic power flow control is not limited to GTI with purely inductive output impedance.

B. Stability analysis

Theorem 1. *Consider the closed-loop system consisting of GTI delivering power to the grid (7) and (8), and the UDE-based dynamic power flow control laws (19) and (20). If the filters $G_{pf}(s)$ and $G_{qf}(s)$ are chosen as strictly proper stable filters with unity gain and zero phase shift over the spectrum of the lumped uncertain terms $\triangle_p$ (9) and $\triangle_q$ (10) and zero gain elsewhere, then the closed-loop system is asymptotically stable, which guarantees stable power delivering of GTI to the grid.*

Proof: When the estimated terms $\hat{\triangle}_p$ (15) and $\hat{\triangle}_q$ (16) are adopted to replace $\triangle_p$ in (13) and $\triangle_q$ in (14), then the error dynamics (11) and (12) become

$$\begin{aligned} \dot{e}_p &= -K_p e_p - \tilde{\triangle}_p, \quad (21) \\ \dot{e}_q &= -K_q e_q - \tilde{\triangle}_q, \quad (22) \end{aligned}$$

where

$$\begin{aligned} \tilde{\triangle}_p &\triangleq \triangle_p - \hat{\triangle}_p \\ \tilde{\triangle}_q &\triangleq \triangle_q - \hat{\triangle}_q \end{aligned}$$

are the estimated error of uncertainty terms. According to (15) and (16), the estimated errors are

$$\begin{aligned} \tilde{\triangle}_p &= \triangle_p * L^{-1}\left\{1 - G_{pf}(s)\right\}, \quad (23) \\ \tilde{\triangle}_q &= \triangle_q * L^{-1}\left\{1 - G_{qf}(s)\right\}. \quad (24) \end{aligned}$$

By substituting (23) into (21) and substituting (24) into (22), and taking the Laplace transformation,

$$\begin{aligned} sE_p(s) &= -K_p E_p(s) - \blacktriangle_p(s)\left[1 - G_{pf}(s)\right], \quad (25) \\ sE_q(s) &= -K_q E_q(s) - \blacktriangle_q(s)\left[1 - G_{qf}(s)\right], \quad (26) \end{aligned}$$

where $E_p(s)$, $\blacktriangle_p(s)$, $E_q(s)$ and $\blacktriangle_q(s)$ are the Laplace transform of e_p, $\triangle_p$, e_q and $\triangle_q$, respectively. Then,

$$\begin{aligned} E_p(s) &= -\frac{\blacktriangle_p(s)\left[1 - G_{pf}(s)\right]}{s + K_p}, \quad (27) \\ E_q(s) &= -\frac{\blacktriangle_q(s)\left[1 - G_{qf}(s)\right]}{s + K_q}. \quad (28) \end{aligned}$$

According to (9) and (10), here $\triangle_p$ and $\triangle_q$ are assumed to be bounded with $|\triangle_p| \leq M_p$ and $|\triangle_q| \leq M_q$, as δ is very small in practical case, E and V_o are engineering signals, and Z_o is a non-zero value. Therefore,

$$|\blacktriangle_p(s)| \leq \frac{M_p}{|s|}, \quad |\blacktriangle_q(s)| \leq \frac{M_q}{|s|}.$$

Since the filters $G_{pf}(s)$ and $G_{qf}(s)$ are designed as a strictly-proper stable filter with unity gain and zero phase shift over the spectrum of the lumped uncertain terms $\triangle_p$ and $\triangle_q$ and zero gain elsewhere, respectively, by applying the final value theorem to (27) and (28), there are

$$\begin{aligned} \lim_{t\to\infty} |e_p| &= \lim_{s\to 0} |s \cdot E_p(s)| \\ &\leq \lim_{s\to 0} \left| \frac{M_p\left[1 - G_{pf}(s)\right]}{s + K_p} \right| \\ &= 0, \\ \lim_{t\to\infty} |e_q| &= \lim_{s\to 0} |s \cdot E_q(s)| \\ &\leq \lim_{s\to 0} \left| \frac{M_q\left[1 - G_{qf}(s)\right]}{s + K_q} \right| \\ &= 0. \end{aligned}$$

Therefore, the tracking errors of the system converge to zero and the close-loop system is asymptotically stable. Stable power delivering of GTI to the grid can be achieved. This completes the proof. ■

IV. Experimental results

A. Experimental setup

To verify the UDE-based dynamic power flow control (19) and (20) , a test rig with one Texas Instruments L-inverter delivering power to a AC bus as shown in Fig. 3(a) was built, where the AC bus is generated by a power amplifier with a signal generator. The circuit diagram is shown in Fig. 3(b), where the loads consist of a resistor $R_L = 6.67\ \Omega$ and a capacitor $C_L = 90\ \mu$F. The loads are connected to AC bus directly and the inverter is connected to the AC bus via a switch CB. In order to synchronize the inverter to the AC bus at the initial state, the load voltage V_o after switch CB is measured by the inverter. The parameters of the inverter are given in Table I. The inverter is controlled through the controlCARD of TI F28M35H52C1 micro-controller chip. The measurement data is sent to a desktop through serial communication.

Table I
Inverter parameters.

Parameters	Values	Parameters	Values
L	7 mH	nominal grid frequency	60 Hz
C	1 μF	nominal grid voltage	14 Vrms
V_{DC}	40 V	PWM frequency	19.2 kHz

B. Filter design and parameter selection

The filters in the UDE algorithm should cover the spectrum of disturbances with the unity gain and zero phase shift. Here, $G_{pf}(s)$ and $G_{qf}(s)$ are chosen as the following first-order low-pass filters

$$G_{pf}(s) = \frac{1}{1 + \tau_p s}, \quad G_{qf}(s) = \frac{1}{1 + \tau_q s}, \quad (29)$$

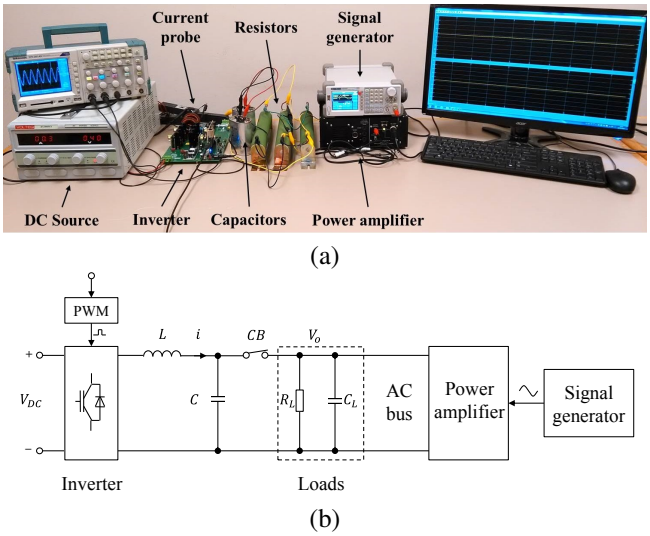

Figure 3. Experimental test rig. (a) Setup (b) Circuit diagram.

with the bandwidth wide enough to cover the spectrum of $\triangle_p$ and $\triangle_q$. Furthermore,

$$\frac{1}{1-G_{pf}(s)} = 1 + \frac{1}{\tau_p s}, \quad \frac{sG_{pf}(s)}{1-G_{pf}(s)} = \frac{1}{\tau_p},$$

and

$$\frac{1}{1-G_{qf}(s)} = 1 + \frac{1}{\tau_q s}, \quad \frac{sG_{qf}(s)}{1-G_{qf}(s)} = \frac{1}{\tau_q}.$$

Therefore, with the low-pass filters (29), the UDE-based control laws (19) and (20) are simplified as

$$\dot{\delta} = \frac{Z_o}{EV_o}\left[\dot{P}_{set} + (K_p + \frac{1}{\tau_p})e_p + \frac{K_p}{\tau_p}\int_0^t e_p dt\right] \quad (30)$$

$$\dot{E} = \frac{Z_o}{V_o}\left[\dot{Q}_{set} + (K_q + \frac{1}{\tau_q})e_q + \frac{K_q}{\tau_q}\int_0^t e_q dt\right]. \quad (31)$$

The control parameters for desired tracking error dynamics and UDE filters are shown in Table II.

Table II
CONTROL PARAMETERS FOR DESIRED TRACKING ERROR DYNAMICS AND UDE FILTERS

Parameters	Values	Parameters	Values
K_p	5	K_q	10
τ_p	0.1 s	τ_q	0.05 s
P_{set}	15 W	Q_{set}	-5 Var

C. System performance

Initially, the grid is set at the nominal frequency 60 Hz and the nominal grid voltage 14 Vrms through the signal generator. The real power is set at $P_{set} = 15$ W, and the reactive power as $Q_{set} = -5$ Var. Then, the grid frequency is stepped up to 60.1 Hz at $t = 5$ s. The grid voltage is stepped down to 13 Vrms at $t = 10$ s. The tuning of both grid frequency and grid voltage is set by the signal generator.

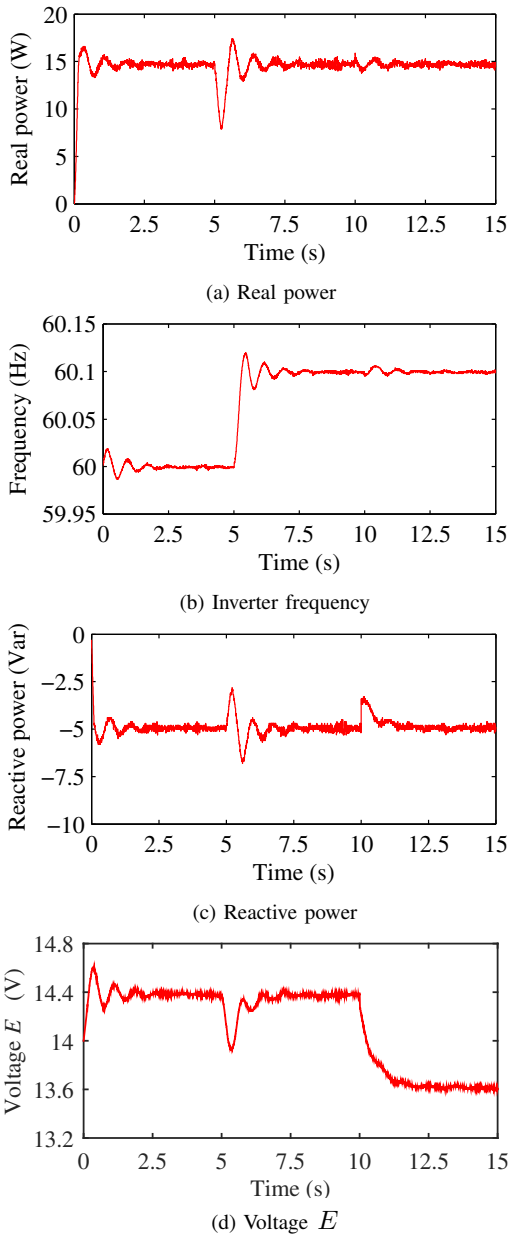

Figure 4. Experimental results

The system response of the proposed UDE-based dynamic power flow control (19) and (20) with the parameters setting in Table II are shown in Fig. 4, including real power response in Fig. 4(a), reactive power response in Fig. 4(c). The inverter frequency and voltage E are shown in Fig. 4(b) and in Fig. 4(d) respectively. Initially, the load voltage V_o is measured by the inverter for synchronization using the zero-crossing method [1], then the inverter starts to deliver the real power and reactive power. This initial synchronization is disabled when the inverter is connected to the grid. The real power and reactive power reach the stable status with $P = 15$ W in Fig. 4(a) and $Q = -5$ Var in Fig. 4(c) quickly. The inverter frequency is within 60 Hz in Fig. 4(b) and voltage E is about $E = 14.4$ Vrms. The UDE-based dynamic power flow control can achieve accurate real power and reactive power output

regulation effectively.

At $t = 5$ s, the grid frequency is changed to 60.1 Hz. There are some oscillations in real power in Fig. 4(a) and reactive power in Fig. 4(c). Both of them converge to the stable status within 2 s. The inverter frequency is changed to 60.1 Hz quickly after some oscillations in Fig. 4(b) without the grid information from an extra synchronization unit. Corresponding response of the voltage E is shown in Fig. 4(d). At $t = 10$ s, the grid voltage is changed to 13 V_{rms}. The reactive power in Fig. 4(c) has a small spike but converges to the stable status within 2 s, and the voltage E in Fig. 4(d) automatically changes to 13.6 V_{rms} within 2 s. The real power in Fig. 4(d) and inverter frequency almost remain the same.

The experimental results show that the external grid disturbance (variations of grid frequency and grid voltage) can be compensated automatically by the UDE-based dynamic power flow control. Also the self-synchronization can be achieved without an extra synchronization unit when the inverter is connected to the grid in the presence of the disturbances from the grid.

V. Conclusion

In this paper, an uncertainty and disturbance estimator (UDE)-based dynamic power flow control has been proposed for grid-tied inverters (GTI) to achieve output power regulation. The power delivering dynamics has been introduced based on the power delivering equations with both frequency dynamics and voltage dynamics being considered. Then the UDE algorithm has been adopted to regulate both output voltage and output frequency for accurate real power and reactive power control. The asymptotic stability has been analyzed for the UDE-based dynamic power flow control. The effectiveness of the proposed approach has been validated experimentally. The self-synchronization can be achieved without an extra synchronization unit when the inverter is connected to the grid in the presence of the disturbances from the grid. Although the UDE-based dynamic power flow control was developed based on the single phase GTI in this paper, the results can be further extended to the three-phase GTI.

Acknowledgment

The authors would like to thank Texas Instruments for the donation of one inverter kit TMDSHV1PHINVKIT.

References

[1] Q.-C. Zhong and T. Hornik. *Control of Power Inverters in Renewable Energy and Smart Grid Integration*. Wiley-IEEE Press, 2012.

[2] S. K. Sul. *Control of Electric Machine Drive Systems*. Wiley-IEEE Press, 2011.

[3] M. Prodanovic and T. C. Green. Control and filter design of three-phase inverters for high power quality grid connection. *IEEE Trans. Power Electron.*, 18(1):373–380, Jan. 2003.

[4] Z. Liu, J. Liu, and Y. Zhao. A unified control strategy for three-phase inverter in distributed generation. *IEEE Trans. Power Electron.*, 29(3):1176–1191, Mar. 2014.

[5] Q.-N. Trinh and H.-H. Lee. An enhanced grid current compensator for grid-connected distributed generation under nonlinear loads and grid voltage distortions. *IEEE Trans. Ind. Electron.*, 61(12):6528–6537, Dec. 2014.

[6] M. Ashabani and Y. A.-R. I. Mohamed. Novel comprehensive control framework for incorporating VSCs to smart power grids using bidirectional synchronous-VSC. *IEEE Trans. Power Syst.*, 29(2):943–957, Mar. 2014.

[7] S. M. Ashabani and Y. A.-R. I. Mohamed. A flexible control strategy for grid-connected and islanded microgrids with enhanced stability using nonlinear microgrid stabilizer. *IEEE Trans. Smart Grid*, 3(3):1291–1301, Sept. 2012.

[8] Q.-C. Zhong, P.-L. Nguyen, Z. Ma, and W. Sheng. Self-synchronized synchronverters: Inverters without a dedicated synchronization unit. *IEEE Trans. Power Electron.*, 29(2):617–630, Feb. 2014.

[9] T.-F. Wu, C.-H. Chang, L.-C. Lin, G.-R. Yu, and Y.-R. Chang. A D-Σ digital control for three-phase inverter to achieve active and reactive power injection. *IEEE Trans. Ind. Electron.*, 61(8):3879–3890, Aug. 2014.

[10] T. Noguchi, H. Tomiki, S. Kondo, and I. Takahashi. Direct power control of PWM converter without power-source voltage sensors. *IEEE Trans. Ind. Appl.*, 34(3):473–479, May 1998.

[11] M. C. Chandorkar, D. M. Divan, and R. Adapa. Control of parallel connected inverters in standalone AC supply systems. *IEEE Trans. Ind. Appl.*, 29(1):136–143, Jan./Feb. 1993.

[12] M. Dai, M. N. Marwali, J.-W. Jung, and A. Keyhani. Power flow control of a single distributed generation unit. *Power Electronics, IEEE Transactions on*, 23(1):343–352, Jan. 2008.

[13] J. M. Guerrero, J. C. Vasquez, J. Matas, M. Castilla, and L. G. de Vicuna. Control strategy for flexible microgrid based on parallel line-interactive UPS systems. *IEEE Trans. Ind. Electron.*, 56(3):726–736, Mar. 2009.

[14] J. Kim, J. M. Guerrero, P. Rodriguez, R. Teodorescu, and K. Nam. Mode adaptive droop control with virtual output impedances for an inverter-based flexible AC microgrid. *IEEE Trans. Power Electron.*, 26(3):689–701, Mar. 2011.

[15] W. R. Issa, M. A. Abusara, and S. M. Sharkh. Control of transient power during unintentional islanding of microgrids. *IEEE Trans. Power Electron.*, 30(8):4573–4584, Aug. 2015.

[16] Q.-C. Zhong and D. Boroyevich. A droop controller is intrinsically a phase-locked loop. In *Proc. 39th IECON*, pages 5916–5921, Nov. 2013.

[17] H.-P. Beck and R. Hesse. Virtual synchronous machine. In *Proc. 9th Int. Conf. EPQU*, pages 1–6, Oct. 2007.

[18] Q.-C. Zhong and G. Weiss. Static synchronous generators for distributed generation and renewable energy. In *Proc. PSCE*, pages 1–6, Mar. 2009.

[19] Q.-C. Zhong and G. Weiss. Synchronverters: Inverters that mimic synchronous generators. *IEEE Trans. Ind. Electron.*, 58(4):1259–1267, Apr. 2011.

[20] M. A. Torres L., L. A. C. Lopes, L. A. Moran T., and J. R. Espinoza C. Self-tuning virtual synchronous machine: A control strategy for energy storage systems to support dynamic frequency control. *IEEE Trans. Energy Convers.*, 29(4):833–840, Dec. 2014.

[21] Q.-C. Zhong and D. Rees. Control of uncertain LTI systems based on an uncertainty and disturbance estimator. *Journal of Dynamic System, Measurement, and Control, ASME*, 126(4):905–910, Dec. 2004.

[22] J. P. Kolhe, M. Shaheed, T. S. Chandar, and S. E. Taloe. Robust control of robot manipulators based on uncertainty and diturbance estimation. *International Journal of Robust and Nonlinear Control*, 23:104–122, 2013.

[23] B. Ren, Q.-C. Zhong, and J. Chen. Robust control for a class of non-affine nonlinear systems based on the uncertainty and disturbance estimator. *IEEE Trans. Ind. Electron.*, 62(9):5881–5888, Sept. 2015.

[24] B. Ren, Y. Wang, and Q.-C. Zhong. UDE-based control of variable-speed wind turbine systems. *International Journal of Control*. DOI 10.1080/00207179.2015.1126678.

[25] A. E. Fitzgerald, C. Kingsley, and S. D. Umans. *Electric Machinery (Sixth Edition)*. McGraw-Hill, 2003.

[26] F. Dorfler and F. Bullo. Synchronization and transient stability in power networks and nonuniform kuramoto oscillators. *SIAM J. Control Optim.*, 50(3):1616–1642, Jun. 2012.

[27] F. Dorfler, M. Chertkov, and F. Bullo. Synchronization in complex oscillator networks and smart grids. *Proc. Nation. Acad. of Sci.*, 110(6):2005–2010, 2013.